Supporting Information

Disorder Engineering of Undoped TiO_2 Nanotube Arrays for Highly Efficient Solar-driven Oxygen Evolution

Maryam Salari *[a], Seyed Hamed Aboutalebi[b], Ali Aghassi [a], Pawel Wagner [a], Attila J. Mozer [a], Gordon G. Wallace *[a]

[a]ARC Centre of Excellence for Electromaterials Science, Intelligent Polymer Research Institute, University of Wollongong, Wollongong, NSW, 2500, Australia

[b]Institute for Superconducting and Electronic Materials, ARC Centre for Electromaterials Science, University of Wollongong, Wollongong, NSW, 2500, Australia

Experimental procedures:

TiO_2 nanotube arrays (TNTA) have been prepared by anodic oxidation of a Ti foil (99.7% purity, Sigma) acting as an anode and a Pt foil acting as a cathode at 15 V for 17 h at room temperature, followed by annealing at different temperatures ranging from 450 ^{0}C to 650 ^{0}C for 5 h under argon atmosphere. The electrolytes consisted of 0.2 wt% NH_4F dissolved in a mixture of glycerol and di-ionized water (9:1 in volume). The anodic TiO_2 nanotube arrays grown on one side of Ti foil were used as the active material and the other side of the foil and also the edges were isolated by epoxy glue. The morphology and microstructure of the prepared TNTA were investigated by the field emission scanning electron microscopy (FE-SEM; JEOL JSM-7500FA), glancing angle X-ray diffraction (GAXRD; GBC MMA X-ray diffractometer with Cu-Ka radiation, and $2\theta = 7^0$), X-ray photoelectron spectroscopy (XPS; SPECS system with Al-Kα radiation and a pass energy of 20 eV), and photoluminescence spectrometer (PL; Fluorolog, Horiba JobinYvon using a Xenon lamp operating at λ= 250 nm , E= 4.96 eV). PL and XPS curve fitting of was performed using the Origin software employing a Gaussian peak shape and linear fitting, respectively. The spectral base was determined by taking an average of the intensity at the binding energies more negative than -3 eV, representing the level of instrument noise at the energy where there is no photoemission intensity.

Photo-electrochemical measurements were carried out in a three electrodes configuration using a workstation (CHI Instruments) and quartz made H-type cell (Makuhari Rikagaku Garasu Inc.). The working electrodes along with Ag/AgCl (3.5 M NaCl) as the reference electrode were placed in one compartment and a Pt mesh as the counter electrode at the other compartment which was separated by a Nafion 117 membrane (DuPont). Simulated sunlight was obtained by a white light source (Newport, Spectra physics, 50-500 Watts) with a light intensity of 150 $mWcm^{-2}$. A 300 Xe lamp (Perkin-Elmer, CERMAXPE-300BF) was also used as a high power light source for illumination of the amorphous TNTA. A cut-off filter (THOR LABS, Unmounted band-pass coloured glass filters: 315-710 nm) was used for the visible light and coloured region irradiation. The electrochemical measurements were performed in 0.1 M Na_2SO_4 (pH=7) aqueous solution as the electrolyte. Cyclic voltammetry (CV) and linear sweep voltammetry (LSV) tests were carried out in a window potential of 1.5 V initiating from the open circuit potentials of different samples at scan rates of 50 $mV\ s^{-1}$ and 5 mVs^{-1}, respectively. LSV test was performed while the light was chopped off manually at regular intervals. In order to avoid any undesired bubbles inside the electrolyte, pure Ar gas was perched into both H-Cell compartments and bubbled 2 hour before initiating the experiments. Amperometric (i-t) curve was obtained under the light illumination and applied bias of 1.1 V (*vs.* Ag/AgCl) in order to investigate the oxygen evolution using an online gas chromatograph (Shimadzu, GC-8A, Ar carrier).

Free-base porphyrin and Cu-porphyrin were also incorporated on anodic TiO_2 nanotube, (named as TNTA/porphyrin, and TNTA/Cu- porphyrin). The TNTA samples were heated for 2 hours under an argon atmosphere, then, were placed in 0.2 mM porphyrin and Cu-porphyrin solutions dissolved in anhydrous ethanol and kept still in a dark place. After 19 hours, samples were gently rinsed in acetonitrile and dried in a horizontal position. For further electrochemical investigations, the back side of the foil and the edges have been subsequently isolated by epoxy glue.

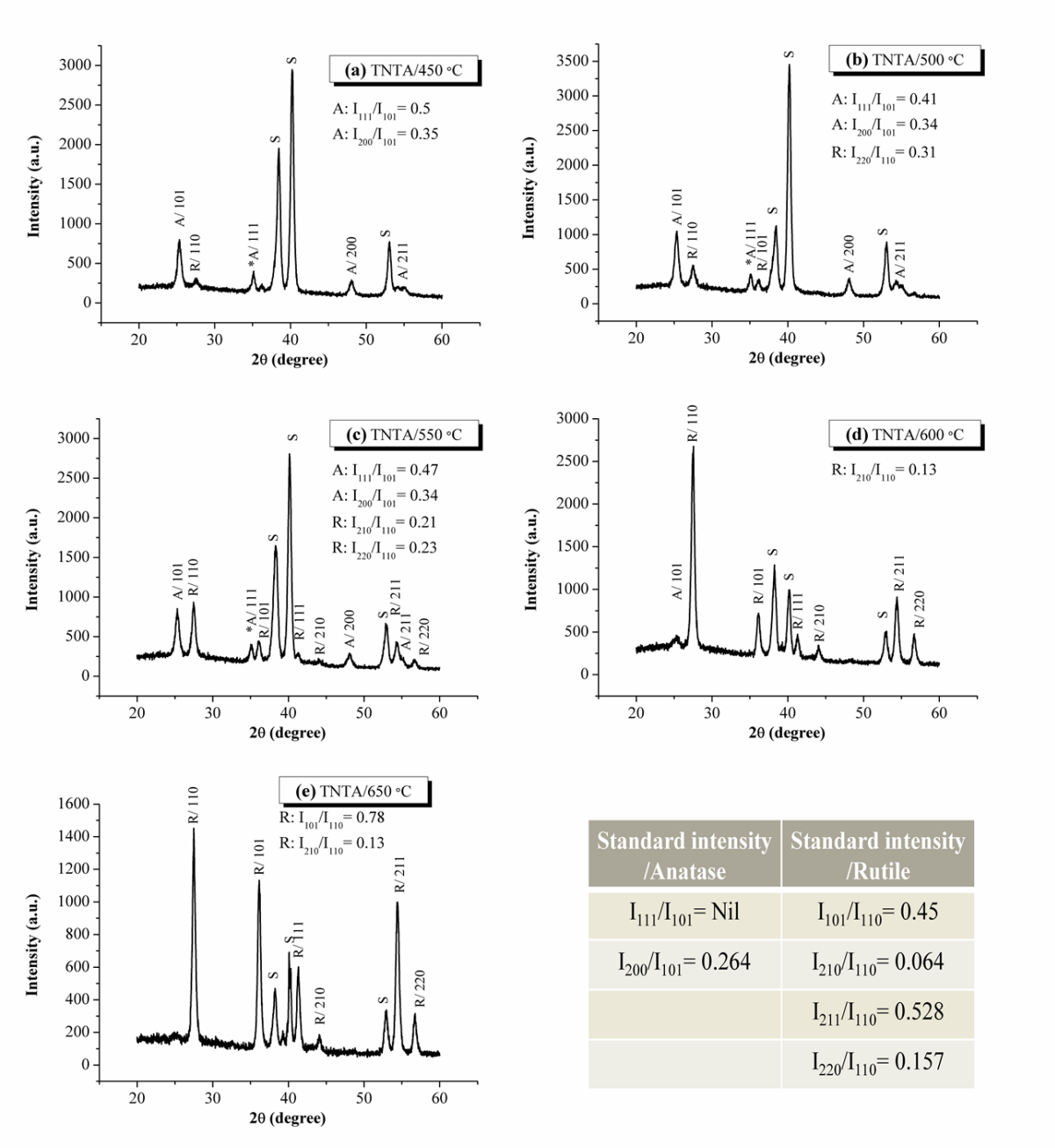

Standard intensity /Anatase	Standard intensity /Rutile
I_{111}/I_{101}= Nil	I_{101}/I_{110}= 0.45
I_{200}/I_{101}= 0.264	I_{210}/I_{110}= 0.064
	I_{211}/I_{110}= 0.528
	I_{220}/I_{110}= 0.157

Fig. S1 XRD patterns of the TiO_2 samples annealed at different temperatures exposed with preferential growth crystal facets (111), (200), and (210).

Photoluminescence (PL) is mostly a surface phenomenon and known as a non-destructive high-sensitivity technique to characterize the optical properties of solid semiconductors. Fig. S2 shows curve fitting of the PL spectra obtained for amorphous TNTA and TNTA/450 ^{0}C-650^{0}C, performed using the Origin software employing a Gaussian peak shape. Annealing at moderate temperatures resulted in broad emissions in the spectral ranging from 364 to 311 nm (3.41 to 3.98 eV) as well as the presence of peak at 466 nm (2.66 eV). Upon annealing at

600 ^{0}C, intensity increase along with change in the shape and position of the PL peaks were observed due to the anatase to rutile phase conversion. Further annealing at higher temperatures; 650 ^{0}C, led to a red-shift in the spectrum. A difference between high-energy bands of TNTA/500 ^{0}C with TNTA 600-650 ^{0}C can be detected due to the different crystal structure and different band structures of anatase and rutile phases. However, the positions of the shallow trap level at λ=466-467 nm is the same, indicating the same origin of the existence of uncoordinated Ti atom /or oxygen vacancies in rutile as well as anatase particles.

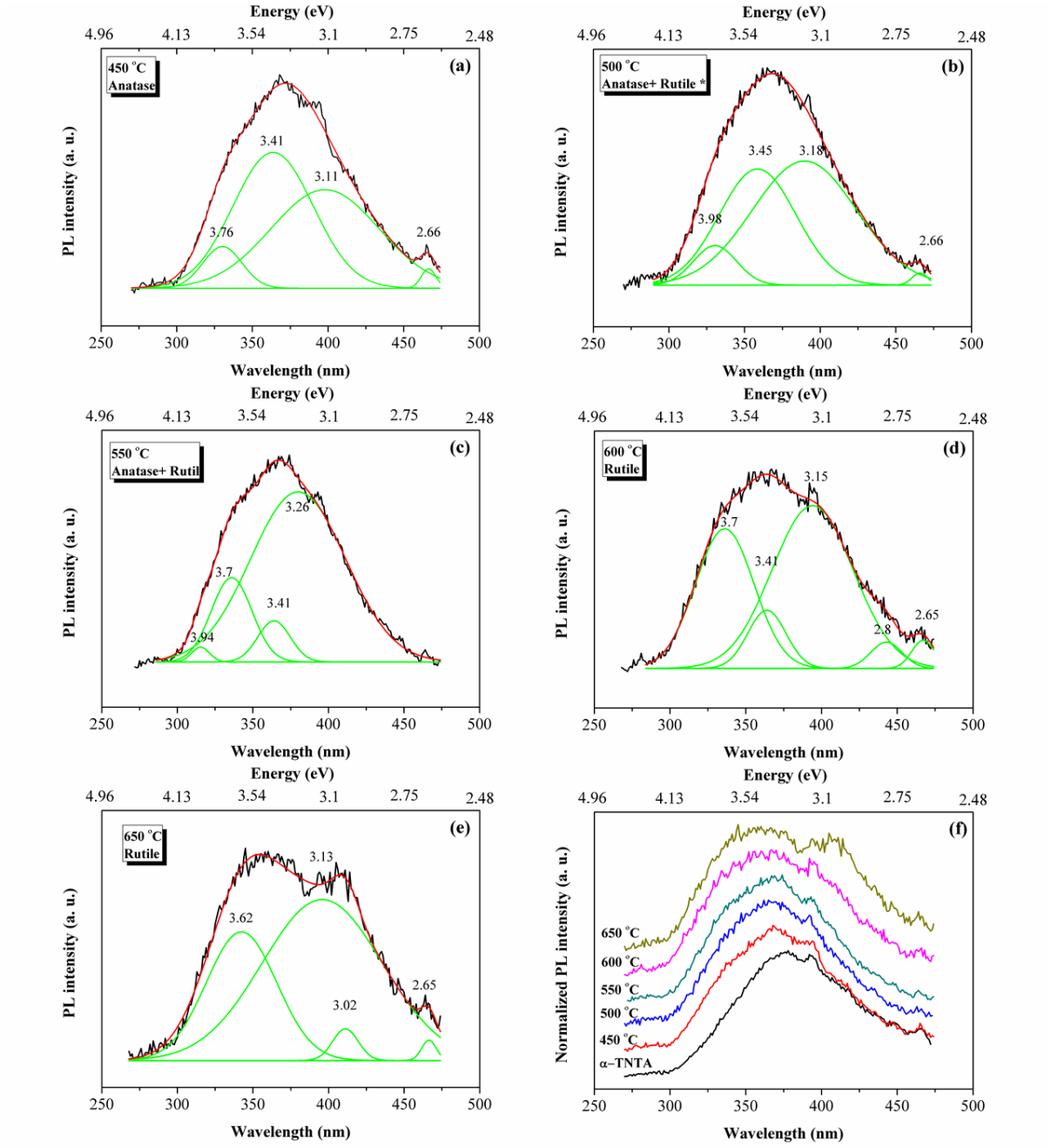

Fig. S2 PL (a-e) spectra obtained for amorphous TNTA and TNTA annealed at different temperatures, the black curve is the experimental results that deconvoluted into eight peaks (green curves), and the red curve is the sum of the deconvoluted peaks, (f) overlaid PL spectra obtained for all samples.

Fig. S3 shows the diffuse reflectance UV-Vis spectra of TNTA annealed at different temperatures. The samples heat treated at lower temperatures show valley at their diffuse reflectance spectra at the wavelength around 370-380 nm. However, the absorbance wavelength of the samples annealed at 600 ^{0}C occurs at 410 nm. The obtained results are in good agreement with the bang gap reported in the manuscript.

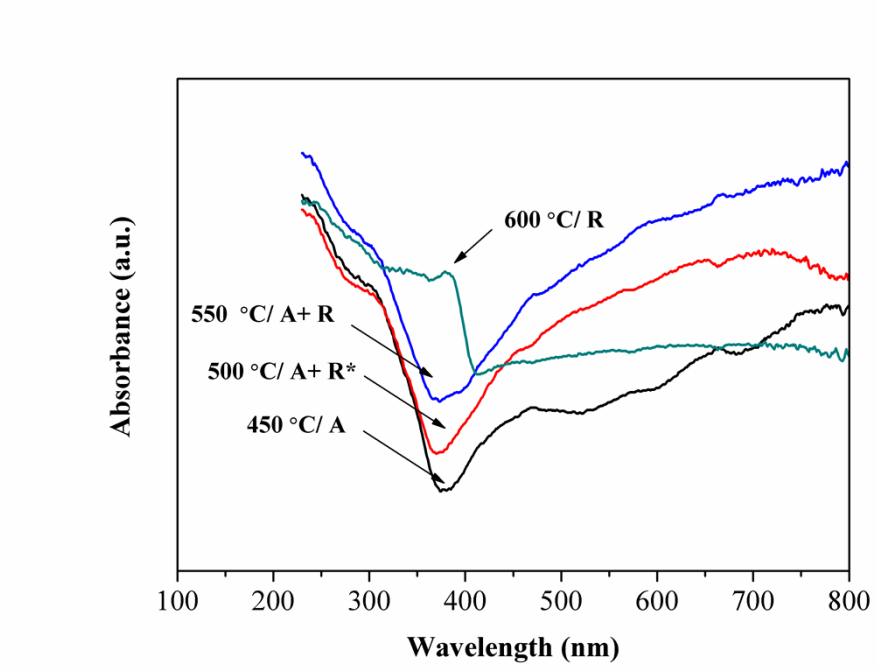

Fig. S3. Diffuse reflectance UV-Vis spectra of TNTA annealed at different temperatures

The stability of water as a function of potential and pH, by use of the Nernst equation, is presented in Fig. S2.Thermodynamically, water splitting involves two half oxidation and reaction process, as follows:

Reduction: $2H^+ + 2e^- \rightarrow H_2$ $E^0 = -0.059pH$

Oxidation: $2H_2O \rightarrow 2O_2 + 4H^+ + 4e^-$ $E^0 = 1.23 - 0.059pH$

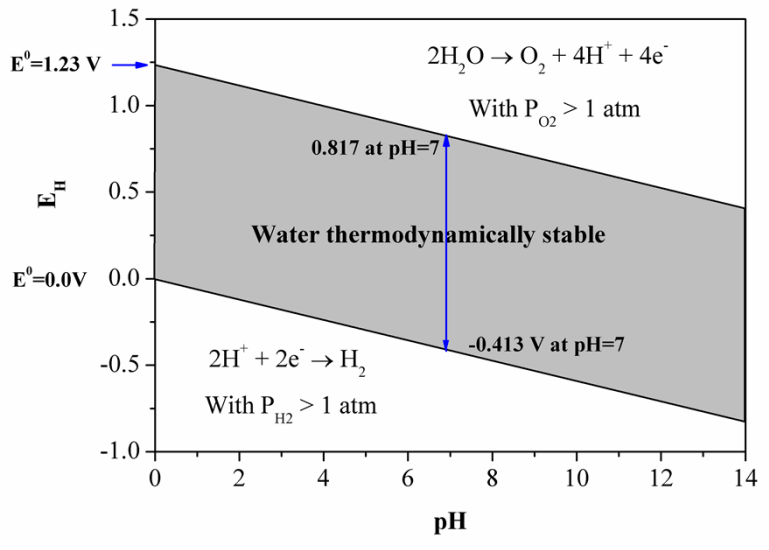

Fig. S4 Pourbaix diagram for water

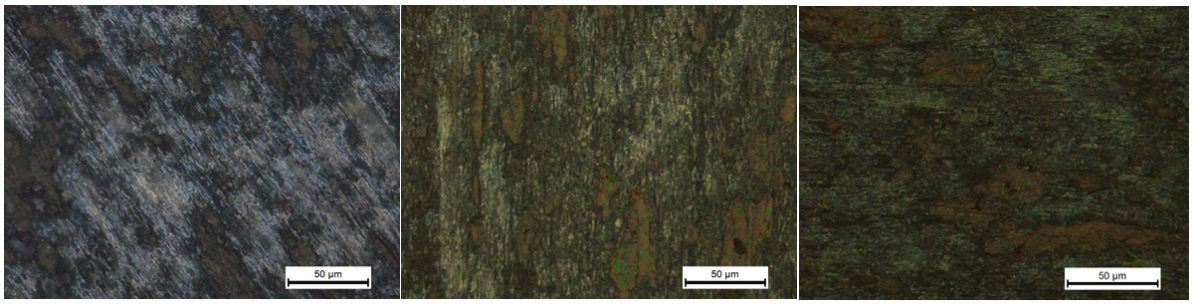

TNTA TNTA + Porphyrin TNTA + Cu-Porphyrin

Fig.S5 Optical microscopy examination of TiO_2 nanotube and TNTA electrodes covered by porphyrins polymers layers.

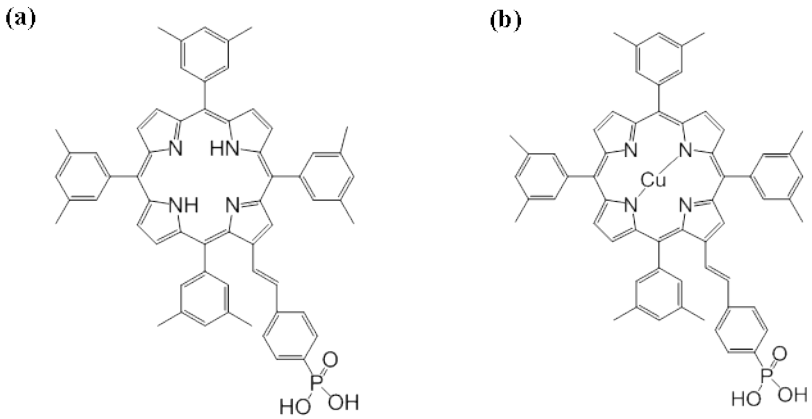

S6. Structures of the porphyrin sensitizers studied in this work; (a) free based porphyrin, and (b) Cu-Porphyrin.

The oxygen gas evolution rate and the faraday efficiency calculated for the bare TNTA and TNTA combined with free base porphyrin, reported in Table S1, show an increase over time even though the current stays constant over the whole experiment duration. We suggest that the error raised from recording the carrier gas flow rate as well as the carrier gas flow fluctuations over the course of experiments are the main reasons responsible for faraday efficiency values over 100%. In addition, the initial faraday efficiency for the bare TNTA and TNTA/porphyrin is calculated to be 51% and 83%, respectively. In our system, GC quantifies the gas accumulated in the head space of the H-cell. It is well established that the gas molecules are closely packed by liquid molecules while in the dissolved state. The molecules of a dissolved gas form a cluster, which is the first step in forming a gas bubble within a liquid. Once a critical cluster is formed, it is growing to a microscopic gas bubble which can leave the liquid and be accumulated in the head space. We suggest that porphyrin is assisting with cluster formation and detachment. The gas quantity measurement used in this study could, therefore, explain the low faraday efficiency calculated for the bare TNTA at the first hour of the experiment. Nevertheless, more importantly, the electrodes can retain current over a long period of time confirming their stable long term performance.

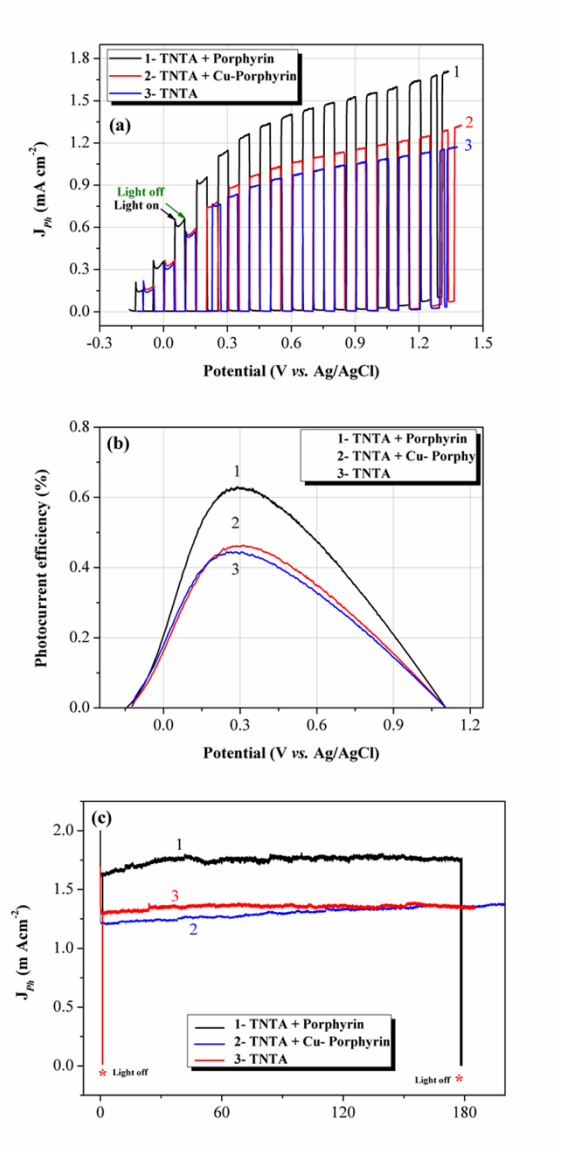

Fig. S7 Comparable (a) linear sweeps voltammetry (LSV) with scan rate of 5 mVs^{-1} under chopped off simulated light powered at 150 mW cm^{-2}, (b) calculated photoconversion efficiencies as a function of the applied potential, and (c) amperometric measurements (*i-v* curve) collected from TNTA with and without porphyrins.

Table S1 Faradaic efficiency of O_2 generation by the TNTA and TNTA/porphyrin

	TNTA		**TNTA/porphyrin**	
Time (hour)	O_2 evolution rate (µl h^{-1})	Faraday efficiency (%)	O_2 evolution rate (µl h^{-1})	Faraday efficiency (%)
1	155	51	328	83
2	277	91	391	99
3	380	125	436	109